THE JOURNAL OF BIOLOGICAL CHEMISTRY
Vol. 275, No. 29, Issue of July 21, pp. 22487–22494, 2000

Printed in U.S.A.

Microtubules Regulate Local Ca^{2+} Spiking in Secretory Epithelial Cells*

Received for publication, November 29, 1999, and in revised form, April 19, 2000
Published, JBC Papers in Press, May 8, 2000, DOI 10.1074/jbc.M909402199

Kevin E. Fogarty‡§, Jackie F. Kidd§¶‖, Angelina Turner¶, Jeremy N. Skepper, Jeff Carmichael‡, and Peter Thorn‡‡**

*From ¶The Department of Pharmacology, Cambridge University, Cambridge CB2 1QJ, United Kingdom, the ‡Biomedical Imaging Group, Department of Physiology, University of Massachusetts Medical School, Worcester, Massachusetts 01650, and the **Multi-Imaging Centre, Department of Anatomy, Cambridge University, Cambridge CB2 3DY, United Kingdom*

The role of the cytoskeleton in regulating Ca^{2+} release has been explored in epithelial cells. Trains of local Ca^{2+} spikes were elicited in pancreatic acinar cells by infusion of inositol trisphosphate through a whole cell patch pipette, and the Ca^{2+}-dependent Cl^- current spikes were recorded. The spikes were only transiently inhibited by cytochalasin B, an agent that acts on microfilaments. In contrast, nocodazole (5–100 μM), an agent that disrupts the microtubular network, dose-dependently reduced spike frequency and decreased spike amplitude leading to total blockade of the response. Consistent with an effect of microtubular disruption, colchicine also inhibited spiking but neither Me_2SO nor β-lumicolchicine, an inactive analogue of colchicine, had any effect. The microtubule-stabilizing agent, taxol, also inhibited spiking. The nocodazole effects were not due to complete loss of function of the Ca^{2+} signaling apparatus, because supramaximal carbachol concentrations were still able to mobilize a Ca^{2+} response. Finally, as visualized by 2-photon excitation microscopy of ER-Tracker, nocodazole promoted a loss of the endoplasmic reticulum in the secretory pole region. We conclude that microtubules specifically maintain localized Ca^{2+} spikes at least in part because of the local positioning of the endoplasmic reticulum.

The localization of signaling complexes is important for the specificity of action of signals within a cell. For example, the tethering of protein kinase A to protein kinase A-associated proteins is used to direct global cAMP signals to specifically regulate proteins linked to protein kinase A-associated protein (1). Another example is Homer, a protein that anchors intracellular release channels close to metabotropic glutamate receptors, and so functionally couples local inositol trisphosphate (IP_3)[1] production with local IP_3 receptors (2). The cytoskeleton is thought to play a role in the cellular positioning of these signaling complexes. In our experiments we sought to determine a role for the cytoskeleton in regional positioning of the Ca^{2+} release apparatus in polarized epithelial cells.

The cytoskeleton maintains the polarization observed in many epithelial cells (3, 4) and, therefore, might be expected to play a role in second messenger signaling cascades. Many epithelia exhibit polarization of Ca^{2+} signaling pathways, including the differential distribution of IP_3 receptors (5, 6), unidirectional Ca^{2+} waves (7, 8), and localized Ca^{2+} responses (9, 10). However, to date, there have been no direct experiments to investigate the role of the cytoskeleton in shaping these signaling elements.

In this study we have used acutely isolated mouse pancreatic acinar cells and established trains of Ca^{2+}-dependent current spikes by the infusion of IP_3 through a whole cell patch pipette. These spikes have previously been shown to be due to localized Ca^{2+} release in the secretory pole region (as identified by the clustering of secretory granules) (9–11). During the trains of IP_3-induced spikes, we tested the effects of agents that affect microfilaments and microtubules. Microfilament disruption transiently affected the response, whereas agents that act on microtubules specifically inhibited the local Ca^{2+} spikes but left the responses to supramaximal carbachol concentrations intact even after an extended time period (up to 1.5 h). We determined that microtubule disruption led to a redistribution of the endoplasmic reticulum away from the secretory pole region. We conclude that microtubules are essential in maintaining local Ca^{2+} spikes, at least in part by locally positioning the endoplasmic reticulum.

EXPERIMENTAL PROCEDURES

Cell Preparation—Fresh isolated mouse pancreatic acinar cells were prepared by collagenase (CLSPA, Worthington, Lakewood, NJ) digestion at 36 °C for 7 min as described previously (12). Cells were plated onto poly-L-ornithine (Sigma, Poole, UK)-coated dishes and used within 3 h of isolation.

Patch Clamp—Whole cell patch clamping was performed with an Axopatch 1D (Axon Instruments) patch clamp amplifier. Pipettes had a resistance of 3–5 MΩ (pipette puller; Brown and Flaming, Sutter Instruments, Novato, CA) and, after breaking through to whole cell had a measured, but uncompensated series resistance of 10–20 MΩ. The pipette solution contained (in millimolar): KCl 140, $MgCl_2$ 1, EGTA or 1,2-bis(2-aminophenoxy)ethane-*N*,*N*,*N*′,*N*′-tetraacetic acid 0.5, KOH-HEPES 10, ATP 2, pH 7.2, inositol 2,4,5-trisphosphate ($Ins(2,4,5)P_3$) 0.01, with the free $[Ca^{2+}]$ fixed at 50 or 100 nM by the addition of $CaCl_2$ at appropriate concentrations (MAXC; Chris Patten, Pacific Grove, CA).

* This work was supported by The Wellcome Trust (Biomedical Research Collaboration Grant to P. T. and R. A. T.), The Wellcome Trust Showcase Award (to P. T. and A. T.), the Medical Research Council (project grant to P. T. and Dr. T. R. Cheek), The Royal Society (project grant to P. T.), National Science Foundation Grants DBI-9200027 and DBI-9724611, and National Institutes of Health Grant R01-5RR09799 (to Walter Carrington supporting K. E. F.). The costs of publication of this article were defrayed in part by the payment of page charges. This article must therefore be hereby marked "*advertisement*" in accordance with 18 U.S.C. Section 1734 solely to indicate this fact.

§ These authors contributed equally to this work.

‖ Recipient of a Biotechnological and Biological Sciences Research Council Studentship.

‡‡ To whom correspondence should be addressed: Dept. of Pharmacology, Cambridge University, Tennis Court Rd., Cambridge CB2 1 QJ, United Kingdom. Tel.: 01223-334017; Fax: 01223-334040; E-mail: pt207@cus.cam.ac.uk.

[1] The abbreviations used are: IP_3, inositol trisphosphate; $Ins(2,4,5)P_3$, inositol 2,4,5-trisphosphate; SP, secretory pole; BP, basal pole.

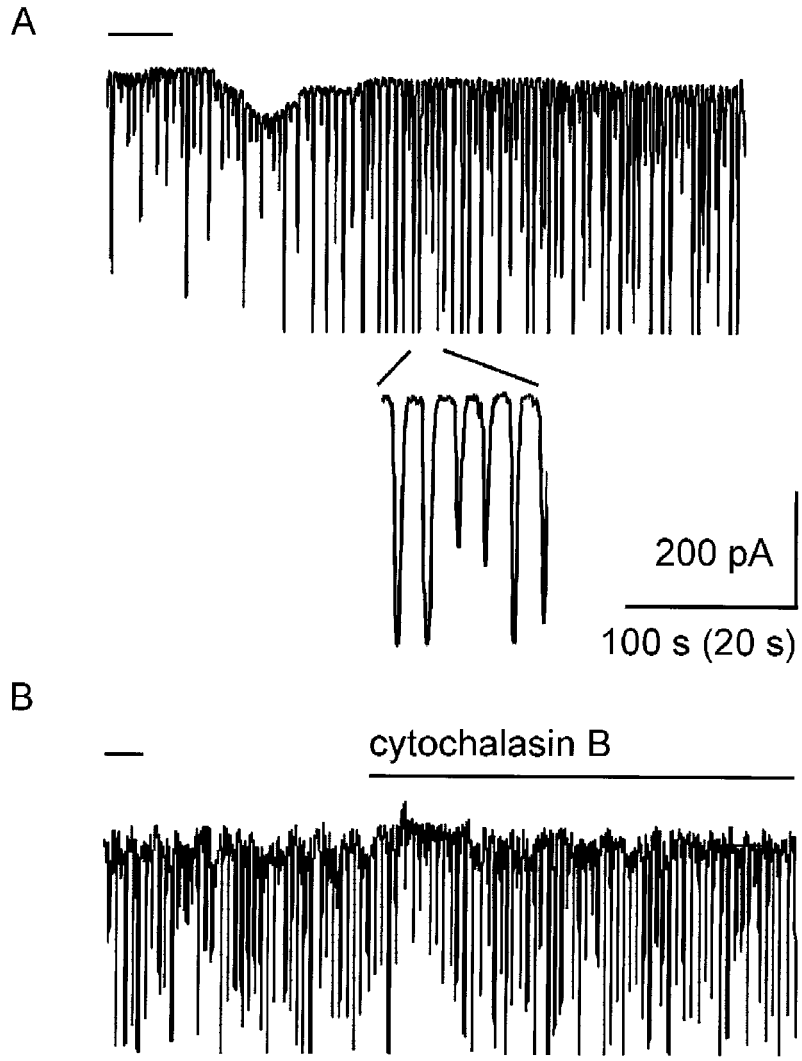

FIG. 1. **Whole cell $Cl_{(Ca)}$ current spikes induced by Ins(2,4,5)P_3 (10 μM) infusion into a single pancreatic acinar cell.** *A*, cells were voltage-clamped to −30 mV, and the downward deflection of current (spikes) is due to the activation of $Cl_{(Ca)}$ channels. The spikes have a duration of 2 s (see *inset*) and have previously been shown to be specifically associated with a local Ca^{2+} signal in the secretory pole region. The *horizontal line* on the *left* of the current records in this and other figures is the zero current line. Small changes in the baseline of the current signal are a reflection of changes in pipette seal resistance or possibly small, slow fluctuations in intracellular Ca^{2+}. Spike activity continued for the length of the whole cell recording with little change in the characteristics of spike amplitude and frequency. These trains of whole cell current spikes were used to test the effects of agents that affect the cytoskeleton. *B*, the addition of cytochalasin B (100 μM) to the bathing solution temporarily decreased the amplitude of the spikes, which thereafter resumed a similar pattern of activity to the control period.

The extracellular solution contained (in millimolar): NaCl 135, KCl 5, $MgCl_2$ 1, $CaCl_2$ 1, glucose 10, NaOH-HEPES 10, pH 7.4. Drugs (all obtained from Sigma) were bolus-applied to the bathing solution, and all experiments were conducted at room temperature (~21 °C). The inclusion of 10–12 μM inositol 2,4,5-trisphosphate (gift from Professor R. Irvine) in the pipette solution elicited a train of short lasting Ca^{2+}-dependent current spikes, previously shown to be a good correlate of localized Ca^{2+} release in the secretory pole of acinar cells (13). The spikes were recorded on a computer using an analogue/digital interface (National Instruments, Austin, TX) and a data acquisition program (J. Dempster). Current amplitudes and current frequency were determined and analyzed with an Excel spreadsheet (Microsoft, OR). In the experiments of Fig. 3 (*inset*), the pipette solution contained (in millimolar): NMDGCl 40, calcium gluconate 1.71, $MgCl_2$ 6.77, *N*-(2-hydroxyethyl)-ethylenediamine-triacetic acid, 10, calculated to give a final free [Ca^{2+}] of 448 nM using the computer algorithm MAXC. The osmolarity was adjusted with mannitol to 300 mOsm. In the experiments of Fig. 3 (*inset*), cells were whole cell voltage-clamped at a potential of −38 mV and voltage steps made in 10 mV increments between −68 and +82 mV. Currents were sampled at 2 kHz, and the peak current amplitudes for each voltage step were recorded as the mean over a 100-ms period at the end of the 2.5-s pulse.

Ca^{2+} Imaging—Ca^{2+} imaging experiments were performed by inclusion of 40–50 μM Ca^{2+} Green (Molecular Probes, Eugene, OR) in the pipette solution. Cells were illuminated with a visible laser (Annova 70; Coherent, Santa Clara, CA) at 488 nm and imaged through a Nikon 40× UV, 1.2 numerical aperature, oil immersion objective. Full-frame images (128 × 128 pixels) were captured on a cooled charge-coupled device camera (70% quantum efficiency, 5 electrons of readout noise; Lincoln Laboratories, Massachusetts Institute of Technology, Cambridge, MA) with a pixel size of 200 nm at the specimen and at frame rates of up to 500 Hz. After recording on the computer, the data were analyzed with custom software with bleach correction routines and appropriate smoothing. Data was recorded as $\Delta F/F_o$ images ($100 \times (F - F_o)/F_o$), where F is the recorded fluorescence and F_o was obtained from the mean of the first 20 acquired frames.

Immunohistochemistry—Cells were prepared as for the patch clamp experiments and plated onto glass coverslips. Next the cells were incubated for 15–20 min in control extracellular solution, solution containing 1% Me_2SO, or solution containing 100 μM nocodazole. At the end of the incubation period the cells were fixed in 2% paraformaldehyde for 15 min and then quenched with ethanolamine, permeabilized with 0.1% Triton, and washed with phosphate-buffered saline. Primary antibodies, either polyclonal rabbit anti-α-tubulin or monoclonal mouse anti-α-tubulin (Sigma), were incubated for 1 h at room temperature (with 3% bovine serum albumin). The cells were then washed three times before addition of either donkey anti-rabbit or goat anti-mouse secondary antibody conjugated to Oregon Green for 1 h at 4 °C. The cells were then washed three times and mounted. The cell fluorescence was imaged in three dimensions and restored as described previously (14, 15).

Visualizing the Endoplasmic Reticulum—We used two methods to observe the endoplasmic reticulum, both using the Dapoxyl probe ER-Tracker (Molecular Probes). The first method used three-dimensional image reconstruction techniques as described (15) with a microscope (Olympus IX70; Melville, NY), an Olympus PL APO 60 × 1.4 numerical aperature oil immersion objective and a 0.25 μm Z section resolution. After cell preparation we incubated the cells in 100–200 nM ER-Tracker for 20–30 min. The cells were then centrifuged, resuspended in normal extracellular solution, and plated onto glass coverslips. These were then treated with drugs before fluorescence microscopy analysis.

In the second method the cells were prepared in exactly the same way but two-photon excitation microscopy (model TCS-SP-MP; Leica Microsystems, Heidelberg, Germany) was used to record the fluorescence signal. Small groups of cells were selected in phase contrast using an infinity-corrected, 63× water immersion, 1.2 numerical aperature, plan apochromatic lens with a cover glass correction collar and a 225-μm working distance. The ER-Tracker was excited by laser light from a solid state Millenia V-pumped Tsunami Ti/sapphire laser tuned to 800 nm, with a pulse width of 1.3 ps and a repetition rate of 82 MHz. Emitted light was captured with a spectrophotometer detector using a window of 450–700 nm. A series of optical sections, with 1-μm increments between images, was taken through the cells to build up a three-dimensional picture of the fluorescence distribution. Drugs were bath-applied after the first series of optical sections had been captured, and further series were captured every 5 min for up to 40 min.

Image analysis was performed using the computer program Lucida (Kinetic Imaging, Liverpool, UK). We measured the average fluorescence in secretory pole (SP) and basal pole (BP) regions (within regions of about 5-μm diameter) and expressed them as a ratio (SP/BP). For each cell, all values were expressed as a percentage of the initial ratio obtained at time 0. The SP/BP ratio, obtained from the same regions, was then followed over time to give an indication of regional changes in fluorescence.

RESULTS

We whole cell patch clamped single mouse pancreatic acinar cells and established a train of Ca^{2+} spikes by the infusion of 10–12 μM $Ins(2,4,5)P_3$ through the pipette solution. Previous work has shown that the activation of $Cl_{(Ca)}$ current spikes are a faithful record of a local secretory pole Ca^{2+} signal (10, 16, 17); therefore, we recorded the whole cell currents as a convenient measure of the regional Ca^{2+} spikes. The injection of $Ins(2,4,5)P_3$ circumvents cell surface receptors and allows the direct study of the mechanisms of IP_3-dependent Ca^{2+} release. Typically, once the whole cell has been established and, after a short period of equilibration (~1 min), a train of $Cl_{(Ca)}$ spikes are established that continue for the lifetime of the whole cell (up to 40 min, Fig. 1*A*).

The secretory pole region of acinar cells, *i.e.* the region where the Ca^{2+} spikes are localized, has an extensive network of microfilaments (18). To test for a role of microfilaments in the mechanism of the generation of the Ca^{2+} spikes, we applied cytochalasin B during an IP_3-induced spike train (Fig. 1*B*). Consistently, we observed that, on addition of 100 μM cytochalasin B to the bathing solution, there was a transient reduction of spike amplitude (Fig. 1*B*, $n = 3$). However, once resumed, the spike activity was apparently no different from the control period before addition of the drug. We conclude that, although the transient inhibition suggests some role, microfilaments are not essential for the maintenance of the local Ca^{2+} spikes.

We then tested the effects of agents known to act on microtubules. Fig. 2*A* shows that the application of nocodazole, an agent known to promote microtubule depolymerization, to the bathing solution led to a cessation of spiking characterized by an initial decrease in spike amplitude followed by a decrease in frequency ($n = 11$). Lower concentrations of nocodazole did not have such rapid effects but instead led to a slower dose-dependent decrease in spike amplitude (Fig. 2*B*). Application of the carrier alone (1% Me_2SO, $n = 3$) had no effect on the spikes.

Given the widespread importance of the microtubular network in cell physiology, the effect of nocodazole treatment might be nonspecific and reflect a general compromise of cell function. However, we showed that, after nocodazole had completely abolished the IP_3-induced spikes, the cells were still able to respond to a supramaximal concentration of carbachol (Fig. 3, 1 mM carbachol, $n = 3$). In fact, we found in other experiments that this supramaximal carbachol response, measured using Ca^{2+} fluorescence techniques, was still maintained after 1.5 h (maximum tested) of nocodazole treatment ($n = 4/5$ cells; 1 cell showed no response, data not shown).

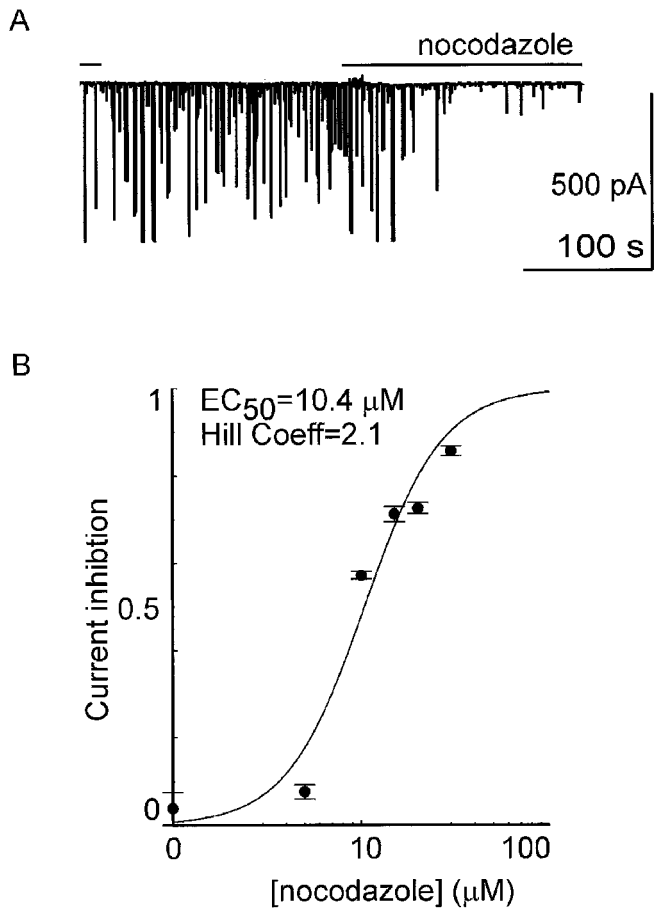

FIG. 2. *A*, after establishment of a train of spikes the bath application of 100 μM nocodazole led to a rapid decrease in spike amplitude followed by a decrease in frequency. *B*, the effects on spike amplitude were measured by cumulative dose-response experiments. In these experiments nocodazole was applied and the amplitude of the spikes recorded. After they had reached a stable level, the spike amplitude was measured. Then higher concentrations of nocodazole were added, and, again after reaching a stable amplitude, the spike size was measured. The results showed a dose-dependent effect of nocodazole on spike amplitude with an approximate IC_{50} of 10.4 μM and a Hill coefficient of 2.1.

The above experiments indicate a specific effect of nocodazole, but in our experiments nocodazole might be directly affecting the $Cl_{(Ca)}$ currents and not the underlying Ca^{2+} signal. We addressed this issue in two ways. First, we directly activated the $Cl_{(Ca)}$ current by the infusion of an intracellular solution containing 448 nM free Ca^{2+} via the whole cell patch pipette. The current-voltage relationships obtained before and after 100 μM nocodazole (Fig. 3, *inset*, $n = 3$) showed no difference in amplitude. Second, we combined patch clamp and Ca^{2+} imaging experiments and directly measured the local secretory pole Ca^{2+} response. Nocodazole (25 μM) reduced the $Cl_{(Ca)}$ current spike amplitude, and this was associated with a reduction in the cytosolic Ca^{2+} rise time and amplitude (Fig. 4, $n = 3$). We conclude that nocodazole specifically affects the local Ca^{2+} spike and not the $Cl_{(Ca)}$ current.

These experiments indicate that nocodazole acts on the mechanism of generation of the local secretory pole Ca^{2+} spike. From the known actions of nocodazole it is implied that its effects are mediated by disruption of the microtubular system. To test this we looked for consistency of action of other agents known to act on microtubules. Colchicine application consistently led to a decrease in spike amplitude (Fig. 5*A*, $n = 4$), and in two cells a decrease in frequency resulted. The effects of colchicine were

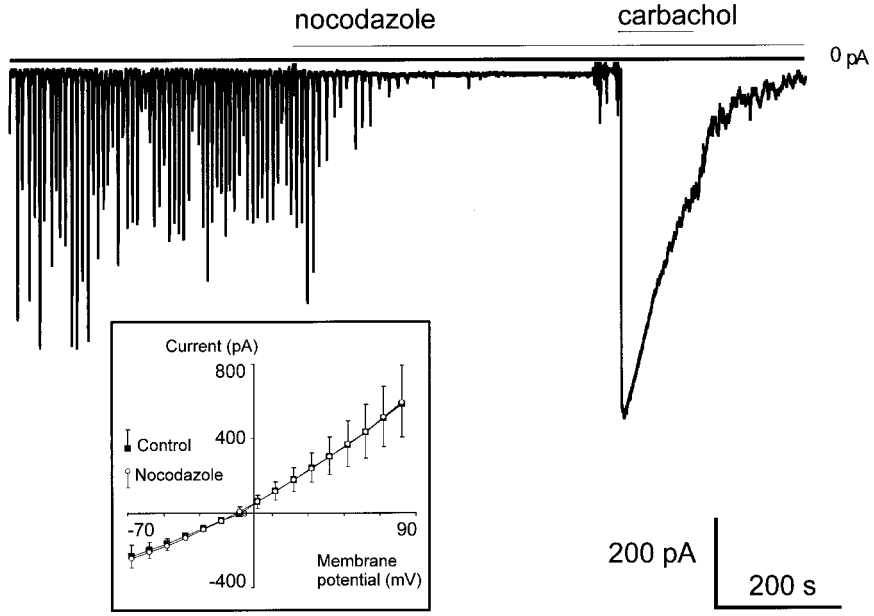

FIG. 3. **Application of nocodazole (100 μM) abolished the train of IP_3-induced spikes, but the subsequent bath application of a supramaximal concentration of the muscarinic agonist carbachol (1 mM) led to a rapid and reversible $Cl_{(Ca)}$ current response.** *Inset*, current-voltage relationships obtained from three cells demonstrate that nocodazole has no direct effect on the $Cl_{(Ca)}$ current. The graph shows the mean and the standard error (*downward error bars* for nocodazole data, *upward* for control data).

slower in onset than nocodazole, with observable effects of colchicine on spike amplitude found at around 3 min after drug application. This is probably a reflection of the action of colchicine, which only binds to free tubulin and does not act directly on tubulin polymerized within microtubules (taxol and nocodazole act on polymerized tubulin) (19). A higher concentration of colchicine (200 μM) blocked the spikes ($n = 3$). A demonstration that these effects were likely to be specific to an action on the microtubular system is shown by the lack of effect of β-lumicolchicine (100 μM; Fig. 5, $n = 5$), a compound with similar structure to colchicine that has no action on tubulin (20).

Another agent that affects microtubules is taxol. Taxol binds to, and stabilizes, microtubules, and we might therefore expect some effect on the Ca^{2+} signal. The addition of 10 μM taxol to the bathing solution led to a loss of spiking (Fig. 6*A*, $n = 6$). In some cells taxol led to an immediate transient increase in the $Cl_{(Ca)}$ current before abolition of the response (Fig. 6*B*, $n = 3/5$). As with the nocodazole effects, after application of taxol, supramaximal concentrations of carbachol were still able to evoke a response (Fig. 6*B*, $n = 3$), indicating the cells were still viable. Furthermore, the current-voltage relationships obtained before and after 10 μM taxol ($n = 3$, data not shown) application showed no difference in amplitude.

Our data are therefore consistent with a role for microtubules in the mechanism of local IP_3-dependent Ca^{2+} release from Ca^{2+} stores. Although the microtubular network has been described for pancreatic acinar cells (21–23) from slices of pancreas, it not been shown in the type of isolated cell preparations we used. Therefore, we performed immunolocalization experiments, using an anti-α-tubulin antibody, on isolated cells that were prepared in the same way as for the previous electrophysiological experiments. The results show a complex network of microtubules throughout the cell (Fig. 7*A*, typical of five preparations). In cells that had been treated with nocodazole for 15 min, the microtubular network was less abundant and showed evidence for truncated tubules, rather than continuous microtubule strands (Fig. 7*B*, typical results from three preparations). These experiments show that nocodazole does exert significant effects on the microtubular system in our isolated cells.

We next explored the possible relationship between the microtubule system and the Ca^{2+} release apparatus. It is well known that microtubules are associated with the organization of the endoplasmic reticulum, and this action may be the source of the functional effects we observe. We visualized the endoplasmic reticulum distribution with the specific probe, ER-

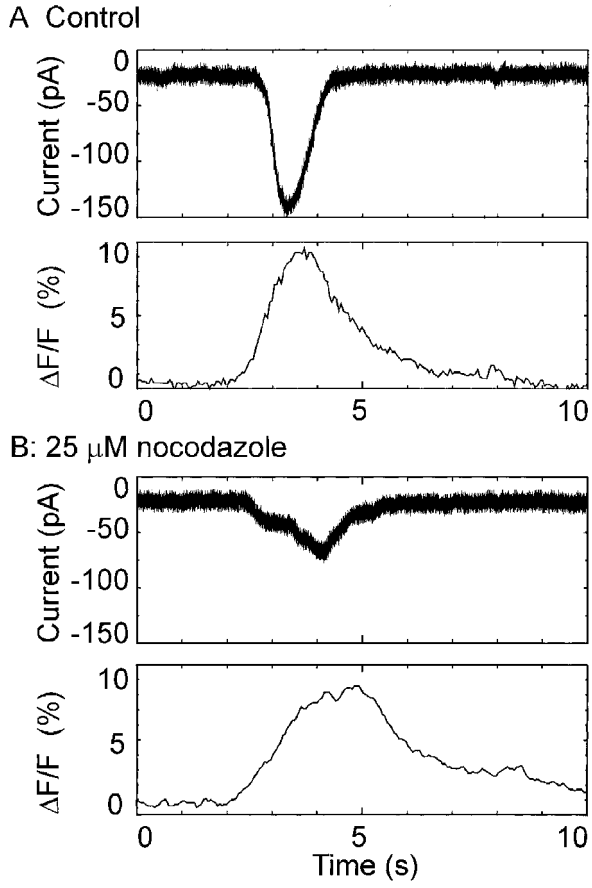

FIG. 4. **Simultaneous measurement of the secretory pole Ca^{2+} signal (using Calcium Green) with the $Cl_{(Ca)}$ whole cell current.** The control experiment in *A* shows that the $Cl_{(Ca)}$ current spike is associated with a rise in the Ca^{2+} signal recorded in the secretory pole. *B*, after treatment with nocodazole (25 μM) the $Cl_{(Ca)}$ current was reduced in amplitude as was the rate of rise and amplitude of the Ca^{2+} response. In cells where the $Cl_{(Ca)}$ current was abolished by nocodazole, no Ca^{2+} spikes were observed.

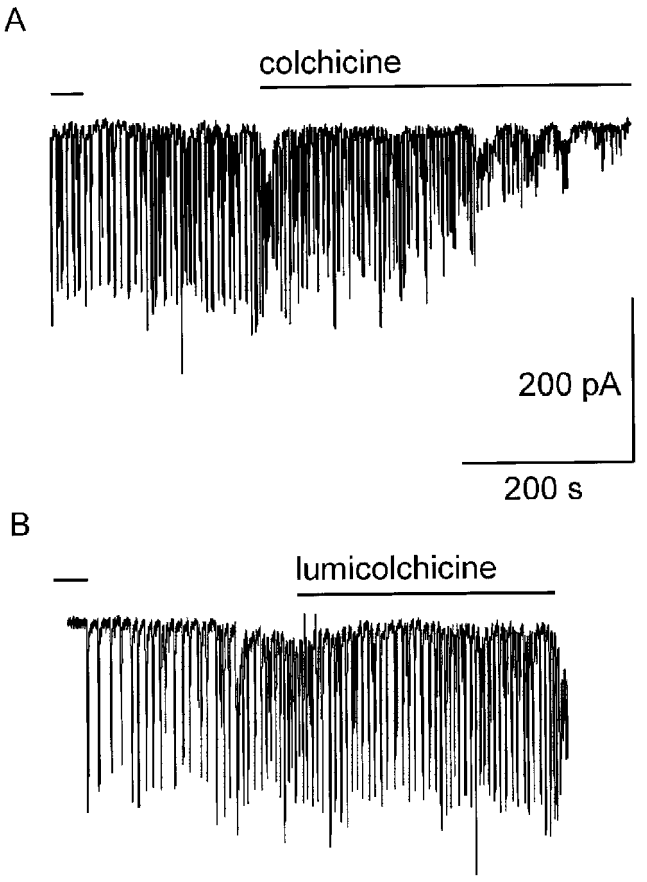

FIG. 5. *A*, bath application of colchicine (100 μM) led to a reduction in spike amplitude and frequency. By comparison to the effects of nocodazole, these effects were delayed in onset. *B*, this effect was not observed in control experiments with β-lumicolchicine, an analogue of colchicine inactive at microtubules.

Tracker. As described previously, the endoplasmic reticulum was distributed throughout the cell (24) but was excluded from the nucleus and the secretory granules (Fig. 8). In control experiments we also studied the distribution of the endoplasmic reticulum resident proteins, calreticulin and BiP, using immunolocalization techniques. Both proteins had a similar apparent cellular distribution to ER-Tracker (data not shown). Two-photon fluorescence imaging methods were used to visualize the endoplasmic reticulum during drug application, using the ER-Tracker dye. We observed changes in the distribution of the endoplasmic reticulum after treatment with nocodazole (100 μM, up to 40 min, n = 7/9 cells; 2 cells showed no apparent change) compared with controls (no drug added, n = 5/6 cells; 1 cell showed small changes in the secretory pole; Fig. 9*A*). Typically, the changes we observed included movement of the unstained region of the nucleus and decreased staining within the secretory pole region (Fig. 9*B*).

To quantify these fluorescence changes, we measured the average signal intensity in a region within the secretory pole (~5-μm diameter) and a region in the basal pole (~5-μm diameter chosen to be away from the nucleus). The ratio of the secretory pole to basal pole signal (SP/BP ratio) was then used as a measure of changes in endoplasmic reticulum distribution. In control conditions we observed no change in the SP/BP ratio over time (Fig. 9*C*). After treatment with nocodazole the ratio decreased significantly ($p < 0.05$ at 10 and 20 min after drug treatment, compared with controls) indicating a reorganization of the endoplasmic reticulum away from the secretory pole.

DISCUSSION

We show agents that act on microtubules have a specific and rapid effect in attenuating IP_3-evoked local Ca^{2+} spikes. Responses to supramaximal agonist concentrations were still observed, even after prolonged treatment with nocodazole, indicating that cell function was still retained and that the microtubular cytoskeleton is not critical for these global Ca^{2+}

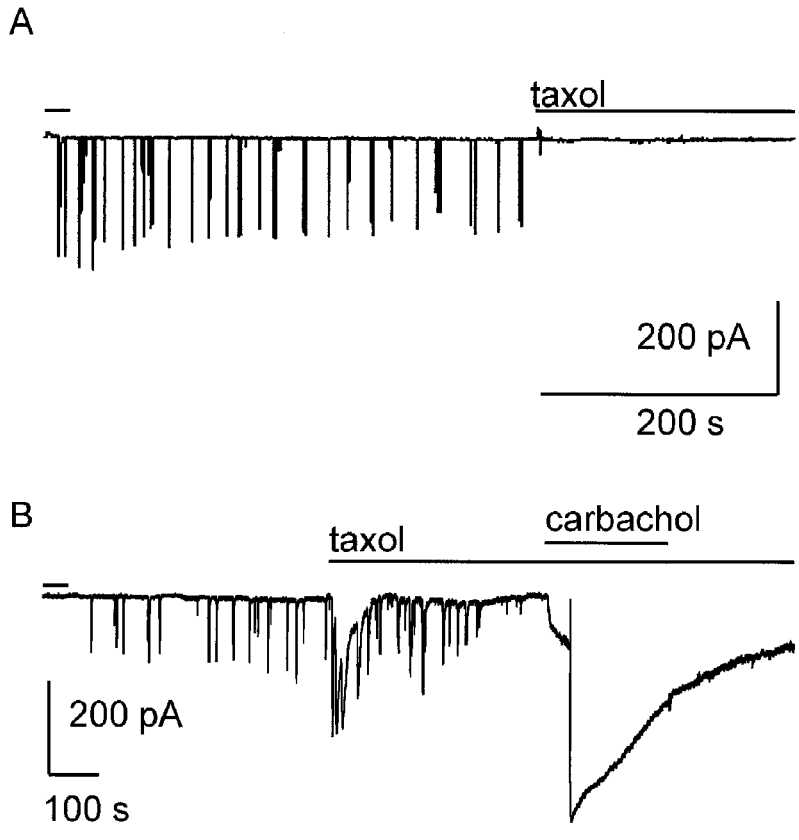

FIG. 6. *A*, bath application of taxol (100 μM) rapidly blocked the train of $Cl_{(Ca)}$ current spikes. In other cells taxol led to a transient increase in spike activity and an increase in the baseline current (*B*) before attenuating spiking. *B*, as with the nocodazole effects we could show that carbachol responses were still maintained after spikes had been abolished.

signals. Microtubular disruption induced a specific decrease of the endoplasmic reticulum in the secretory pole, as visualized by a local loss of ER-Tracker fluorescence. This loss was significant at 10 min after nocodazole treatment, a time course consistent with the effects of nocodazole on the Ca^{2+} spikes. We conclude that the microtubular network specifically maintains local Ca^{2+} responses possibly by local positioning of the endoplasmic reticulum.

There are now a number of recent studies that indicate that the cytoskeleton may play a role in Ca^{2+} signaling processes. Although the cell type and stimulus and signal responses are diverse in these reports, the common thread is a cytoskeletal involvement in signal compartmentalization.

IP_3-evoked Release Compartment—In many cell types, patterns of IP_3-evoked Ca^{2+} release are dependent on local positioning of Ca^{2+} release apparatus (25). In acinar cells apical to basal pole waves and local Ca^{2+} signals are due to polar compartmentalization of IP_3-dependent stores (6, 7, 13). Our work now shows that the functionality of the apical compartment, which generates the local Ca^{2+} spike, is maintained by the microtubular system. This conclusion is based on the consistency of action of agents that target microtubules. Both nocodazole and taxol bind to polymerized tubulin and, respectively, prevent (26) or stabilize (27, 28) microtubule formation. However, colchicine only binds to free tubulin (19, 29) and secondarily interferes with microtubule polymerization. The fact that all these agents inhibit local Ca^{2+} spiking strongly argues for a crucial role of the microtubular system in maintaining the function of Ca^{2+} release sites within the secretory pole region.

If the function of the Ca^{2+} release apparatus is dependent on microtubules, why do we see effects on the local Ca^{2+} spike and not on the carbachol-induced global Ca^{2+} signal? We know that the local Ca^{2+} spike, which we elicited at low IP_3 concentrations (just above threshold), is the reflection of multiple sites of Ca^{2+} release within the apical region that are coordinated together by the action of cytosolic Ca^{2+} (16). Therefore, the architectural arrangement of these release sites within the cell might be an important parameter in the production of the local Ca^{2+} spike. Microtubules could act to position the release sites, and microtubule reorganization might move the sites far

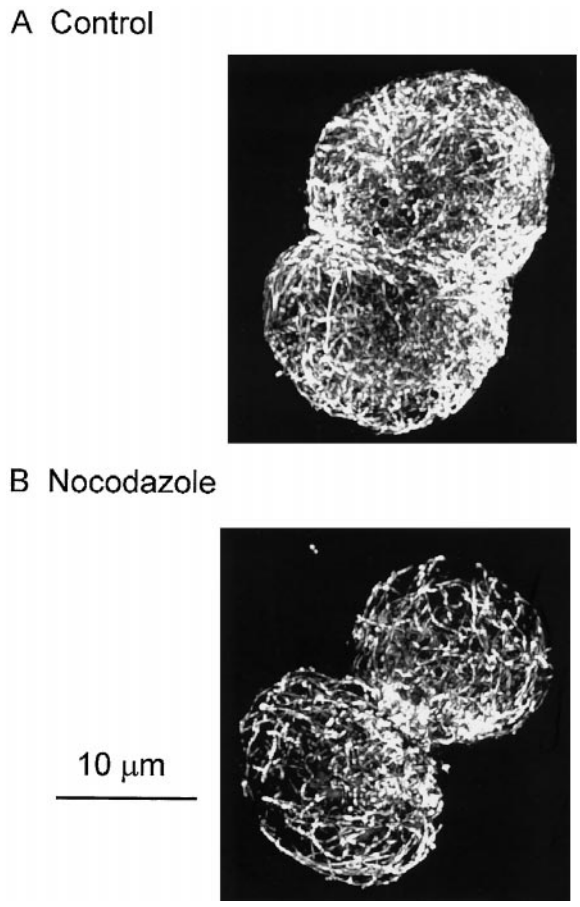

FIG. 7. **Immunolocalization of the microtubules using an antibody raised against α-tubulin.** 36 serial z-sections were taken through the cell and then projected onto the single images shown. *A*, a typical example of a two-cell cluster, a dense network of microtubules with some concentration around the secretory pole. *B*, different cells obtained from the same preparation showed that after treatment with nocodazole the number of microtubules was reduced and those remaining were broken and truncated. *Scale bar*, 10 μm.

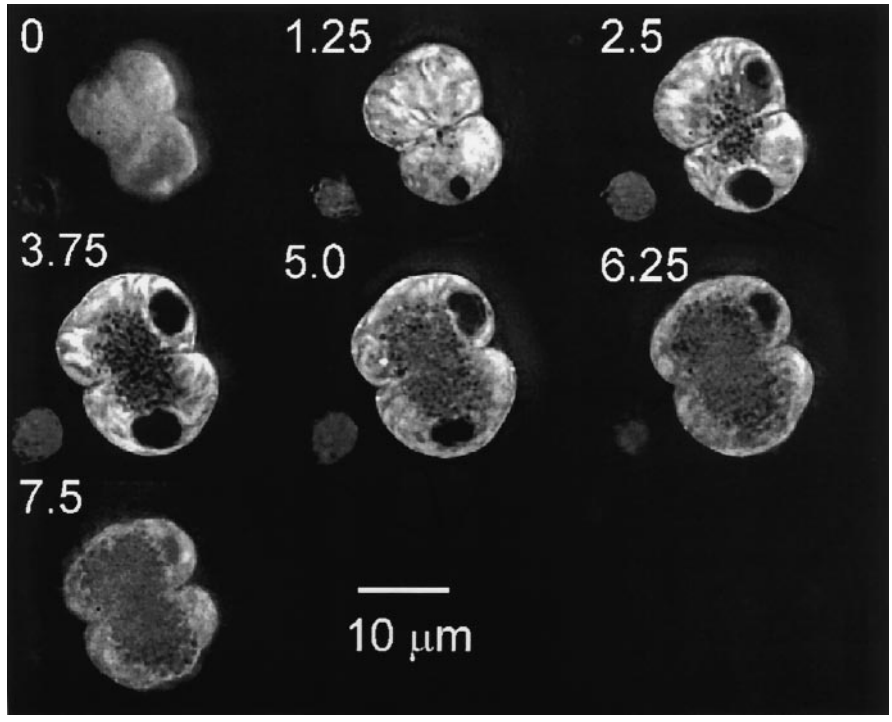

FIG. 8. **Using three-dimensional image reconstruction techniques, the fluorescence signal from the endoplasmic reticulum probe ER-Tracker was localized within a two-cell cluster of acinar cells.** Serial optical sections 1.25 μm apart (identified on the figure) were taken through the cells. The endoplasmic reticulum was found throughout the cell except within the nuclear region and secretory granules.

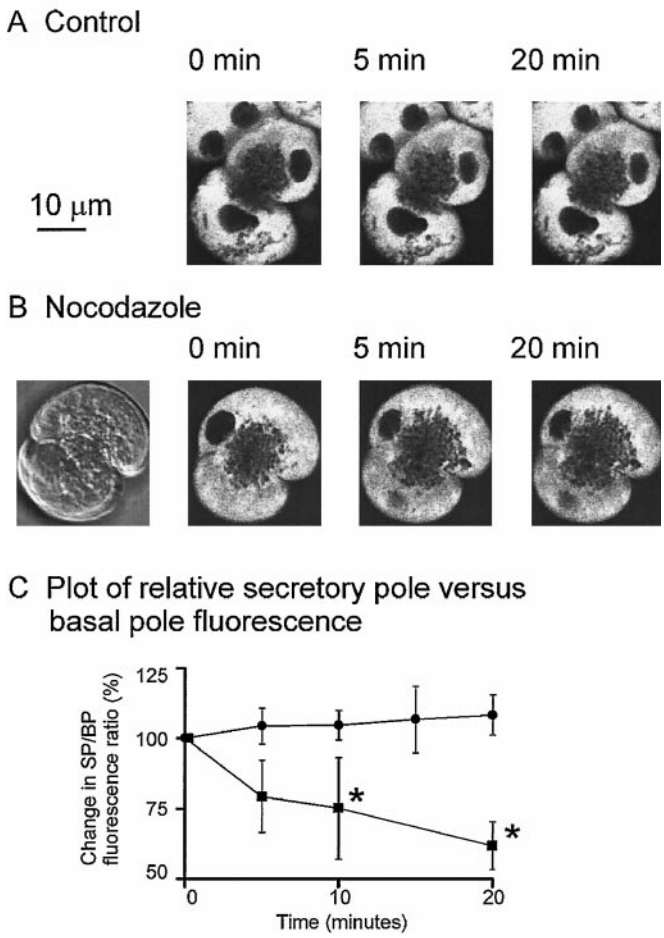

FIG. 9. **Two-photon images of ER-Tracker fluorescence taken from a mid section through an acinar cell cluster.** The endoplasmic reticulum is widely distributed throughout the cell but, as expected, fluorescence is excluded from the nucleus and the secretory granules. Under control conditions (*A*) the pattern of staining did not change when recording over time. In *B*, control images were obtained at 0 min, after which 100 μM nocodazole was added to the bath. Subsequently images were captured at 5 and 20 min after nocodazole treatment. The pattern of fluorescence was observed to change in the secretory pole region and in the position and shape of the excluded fluorescence in the nuclear region ($n = 7/9$, with two cells showing no apparent changes). *C*, the ratio of the mean fluorescence intensity within a 5-μm diameter area in the secretory pole (SP) against a spot of 5-μm diameter in the basal pole (BP) was measured in the same regions over time. Within a single cell, all values were expressed as a percentage of the ratio obtained at time 0. The ratios do not change in control conditions but show a decrease over time in the presence of nocodazole. This decrease is significant (at $p < 0.05$, Student's *t* test) at times 10 and 20 min after the addition of nocodazole, compared with controls.

enough apart such that Ca^{2+} release from one site would not be able to act on an adjacent site to coordinate the signal response via Ca^{2+}-induced Ca^{2+} release. In contrast, the Ca^{2+} release elicited by high agonist concentrations reflects a synchronized global response to saturating IP_3 concentrations. The precise position of Ca^{2+} release sites within the cell would therefore be expected to be of less importance.

A few studies suggest that microtubules underlie the location of Ca^{2+} release within a cell (*e.g.* see Ref. 30). Specific support for a role of microtubules in precisely and locally positioning Ca^{2+} release sites comes from work on endothelial cells. In these cells colchimid treatment for 24 h led to a cellular relocation of caveolin, a protein associated with caveolae, from the cell surface to the interior. Associated with the movement of caveolin was a parallel relocation of sites of Ca^{2+} release (31).

Store-operated Ca^{2+} Entry: Endoplasmic Reticulum Compartment—Modification of the cytoskeleton has been shown to attenuate store-operated Ca^{2+} entry. These experiments have been used as an argument to support a conformational coupling between the IP_3 receptor and the Ca^{2+} entry channel. However, it is not clear at the moment if microtubules or microfilaments play a specific role in this process or if their action is an indirect effect of changes in cell shape. In type 1 astrocytes, microfilament or microtubule disruption abolished a cAMP-mediated up-regulation of Ca^{2+} entry (32), and cytoskeletal disruption was associated with changes in the endoplasmic reticulum, as visualized with ER-Tracker. Abolition of store-operated Ca^{2+} entry has also been seen in HEK293 cells by a calyculin A-mediated production of a cortical actin network (33). In support of a role for microfilaments, their disruption abolishes Ca^{2+} entry into endothelial cells (34). In complete contrast to the above work, Ribeiro *et al.* (35) show that neither microfilament or microtubule disruption affect store-dependent Ca^{2+} entry in fibroblasts, even though they observed dramatic changes in cell shape and endoplasmic reticulum distribution.

What Ribeiro *et al.* (35) have shown is that that 1-h treatment with cytochalasin D or nocodazole abolished agonist-evoked global Ca^{2+} signals in fibroblasts. This effect was not due to a reduction in IP_3 production, a loss of IP_3-evoked Ca^{2+} release, or an effect on Ca^{2+} influx. They explained their data in terms of a role for the cytoskeleton in maintaining a subplasma membrane compartment where phospholipase C, and therefore IP_3 production, is positioned close to the IP_3 receptors. In their view, disruption of the cytoskeleton moves these components far enough apart such that IP_3 degradation becomes significant. Consistent with the idea of a local compartment of IP_3 production, work in polarized epithelial cells suggests that phospholipase C activation in the apical or basal membrane leads to domain-specific responses (36). However, in other cells this is not the case and here it can be shown that IP_3 acts as a global messenger (37). For example, in acinar cells it is clear that agonist action at receptors on the basal pole leads to global elevation in IP_3 and a primary effect on Ca^{2+} release sites at the opposite, secretory (apical) pole (7). In fact, in contrast to Ribeiro *et al.*, evidence from endothelial cells (30, 31, 34), type 1 astrocytes (32), and the work we now present in acinar cells (studying the global Ca^{2+} response) shows that agonists are capable of inducing responses after cytoskeletal disruption.

With reference to our own work, the local Ca^{2+} responses in acinar cells that we have recorded show little dependence on Ca^{2+} influx (38). In our experiments (data not shown) we found that removal of extracellular Ca^{2+} had no acute effects on Ca^{2+} spiking. This indicates that the effects of microtubular disruption we observe are not due to effects on a Ca^{2+} entry mechanism.

Mechanism of Action of Microtubules on Local Ca^{2+} Release in Acinar Cells—The effects we observe indicate that microtubules are important in maintaining the local Ca^{2+} response. However, the link between microtubules and the Ca^{2+} release apparatus is not clear. We consider here two likely potential components of the Ca^{2+} release apparatus, the endoplasmic reticulum and the IP_3 receptor, that might interact with microtubules.

It is well known that endoplasmic reticulum is associated with the microtubular network (39, 40) and potentially involves multiple transport and localization mechanisms (41). The mechanisms for this association remain unclear (42, 43) but lead to the movement of endoplasmic reticulum vesicles along microtubule tracks and association of endoplasmic reticulum

with growing plus ends of microtubules (41). These processes probably do play a role in positioning the endoplasmic reticulum in acinar cells. In support of this, after nocodazole treatment, we show a specific regional reorganization of the endoplasmic reticulum, which we have quantified as a loss of the endoplasmic reticulum in the secretory pole. Furthermore, our study shows that significant effects are seen after 10 min of nocodazole treatment, which is consistent with the rapid time course of the loss of the Ca^{2+} spikes we observe.

Despite the fact that we do observe changes in the distribution of the endoplasmic reticulum, it is difficult to conceive of a microtubule-endoplasmic reticulum interaction, which alone could explain the establishment of local Ca^{2+} responses in acinar cells. The endoplasmic reticulum is widespread throughout the acinar cell with a predominance in the basal pole. Functionally, we know that the endoplasmic reticulum is heterogeneous with local regions of protein exported to the Golgi (44, 45) and other regions specialized for Ca^{2+} release (25). A mechanism for positioning of the Ca^{2+} release apparatus in the apical pole would therefore have to distinguish between endoplasmic reticulum destined for each of the two poles.

In terms of the generation of the local Ca^{2+} signal, interaction between IP_3 receptors and microtubules could provide a direct way for the cell to position the secretory pole Ca^{2+} release apparatus. Disruption of the microtubular network might affect the IP_3 receptor in two ways. First, untethering the IP_3 receptors may lead to a spatial disorganization in the secretory pole region. As speculated above, positioning of Ca^{2+} release sites may be a critical factor in maintaining the local Ca^{2+} spike. Second, uncoupling the IP_3 receptor from the microtubules may more directly affect IP_3 receptor function. In support of an effect on IP_3 receptor function, it has been shown, in *Xenopus* oocyte microsomes, that taxol (but not nocodazole) reduced the effectiveness of IP_3 to evoke Ca^{2+} release (46). This work implies that taxol modifies the function of the IP_3 receptor. Further support for a direct interaction between microtubules and IP_3 receptors comes from experiments in mast cells that showed that the agonist-evoked Ca^{2+} signal was lost after colchicine treatment. This effect was demonstrated to be due to a direct block at the IP_3 receptor (47). Although we did not see block of the agonist-evoked global signals after nocodazole treatment, it is possible that the behavior of the IP_3 receptor (such as affinity for IP_3) may have changed in our experiments. This might lead to our observations of a block of the local response while sparing the global signal.

Microtubule Dynamics during Agonist-evoked Responses—Agonists have been shown to induce changes in the cytoskeleton of acinar cells and play a role in modulating the secretory response (18, 48). These effects may be mediated by a variety of mechanisms. For example, it is known that receptor-dependent activation of cytoskeleton-directed kinases, such as p38 mitogen-activated protein kinase, can modulate the actin microfilament network (49). In addition, second messenger signals may regulate the cytoskeleton. For example, Ca^{2+} (50) or Ca^{2+}-calmodulin can lead to microtubule disassembly (51), an effect that may be modulated by specific microtubule-associated proteins (52). This potential feedback process of Ca^{2+} on the cytoskeleton might be important for microtubule localization in the secretory pole region. Indeed, it is known that calmodulin does translocate to the secretory pole region (53) and, therefore, may well play a role in local microtubule dynamics.

Conclusion—Our data provide functional evidence that the microtubular network plays an important and specific role in the maintenance of local Ca^{2+} spikes. We suggest that this network maintains the position of the Ca^{2+} release apparatus via a local organization of the endoplasmic reticulum.

Acknowledgment—The *in vitro* two-photon imaging studies were carried out in the Multi-Imaging Center on equipment generously provided by the Wellcome Trust.

REFERENCES

1. Gray, P. C., Scott, J. D., and Catterall, W. A. (1998) *Curr. Opin. Neurol.* **8,** 330–4
2. Fagni, L., Chavis, P., Ango, F., and Bockaert, J. (2000) *Trends Neurosci.* **23,** 80–88
3. Mays, R. W., Beck, K. A., and Nelson, W. J. (1994) *Curr. Opin. Cell Biol.* **6,** 16–24
4. Caplan, M. J. (1997) *Am. J. Physiol.* **272,** 4 Pt 2, F425–F429
5. Nathanson, M. H., Fallon, M. B., Padfield, P. J., and Maranto, A. R. (1994) *J. Biol. Chem.* **269,** 4693–4696
6. Lee, M. G., Xu, X., Zeng, W., Diaz, J., Wojcikiewicz, R. J., Kuo, T. H., Wuytack, F., Racymaekers, L., and Muallem, S. (1997) *J. Biol. Chem.* **272,** 15765–15670
7. Kasai, H., and Augustine, G. J. (1990) *Nature* **348,** 735–738
8. Nathanson, M. H., Padfield, P. J., O'Sullivan, A. J., Burgstahler, A. D., and Jamieson, J. D. (1992) *J. Biol. Chem.* **267,** 18118–18121
9. Kasai, H., Li, Y. X., and Miyashita, Y. (1993) *Cell* **74,** 669–677
10. Thorn, P., Lawrie, A. M., Smith, P. M., Gallacher, D. V., and Petersen, O. H. (1993) *Cell* **74,** 661–668
11. Thorn, P., Moreton, R., and Berridge, M. (1996) *EMBO J.* **15,** 999–1003
12. Thorn, P., and Petersen, O. H. (1992) *J. Gen. Physiol.* **100,** 11–25
13. Thorn, P. (1996) *Cell Calcium* **20,** 203–214
14. Dictenberg, J. B., Zimmerman, W., Sparks, C. A., Young, A., Vidair, C., Zheng, Y., Carrington, W., Fay, F. S., and Doxsey, S. J. (1998) *J. Cell Biol.* **141,** 163–174
15. Carrington, W. A., Lynch, R. M., Moore, E. D., Isenberg, G., Fogarty, K. E., and Fay, F. S. (1995) *Science* **268,** 1483–1487
16. Kidd, J. F., Fogarty, K. E., Tuft, R., and Thorn, P. (1999) *J. Physiol.* **520,** 187–201
17. Fogarty, K. E., Kidd, J. F., Tuft, R. A., and Thorn, P. (2000) *Biophys. J.* **78,** 2298–2306
18. Muallem, S., Kwiatkowska, K., Xu, X., and Yin, H. L. (1995) *J. Cell Biol.* **128,** 589–598
19. Bergen, L. G., and Borisy, G. G. (1986) *J. Cell. Biochem.* **30,** 11–18
20. Salmon, E. D., McKeel, M., and Hays, T. (1984) *J. Cell Biol.* **99,** 1066–1075
21. Achler, C., Filmer, D., Merte, C., and Drenckhahn, D. (1989) *J. Cell Biol.* **109,** 179–189
22. Marlowe, K. J., Farshori, P., Torgerson, R. R., Anderson, K. L., Miller, L. J., and McNiven, M. A. (1998) *Eur. J. Cell Biol.* **75,** 140–152
23. Kurihara, H., and Uchida, K. (1987) *Histochemistry* **87,** 223–227
24. van de Put, F. H. M. M., and Elliott, A. C. (1996) *J. Biol. Chem.* **271,** 4999–5006
25. Berridge, M. J. (1997) *J. Physiol.* **499,** 291–306
26. Samson, F., Donoso, J. A., Heller-Bettinger, I., Watson, D., and Himes, R. H. (1979) *J. Pharm. Exper. Therap.* **208,**(3), 411–7
27. Collins, C. A., and Vallee, R. B. (1987) *J. Cell Biol.* **105,** 6 Pt 1, 2847–2854
28. Wilson, L., Miller, H. P., Farrell, K. W., Snyder, K. B., Thompson, W. C., and Purich, D. L. (1985) *Biochemistry* **24,** 5254–5262
29. Vandecandelaere, A., Martin, S. R., Schilstra, M. J., and Bayley, P. M. (1994) *Biochemistry* **33,** 2792–2801
30. Graier, W. F., Paltauf-Doburzynska, J., Hill, B. J., Fleischhacker, E., Hoebel, B. G., Kostner, G. M., and Sturek, M. (1998) *J. Physiol.* **506,** 109–125
31. Isshiki, M., Ando, J., Korenaga, R., Kogo, H., Fujimoto, T., Fujita, T., and Kamiya, A. (1998) *Proc. Natl. Acad. Sci. U. S. A.* **95,** 5009–5014
32. Grimaldi, M., Favit, A., and Alkon, D. L. (1999) *J. Biol. Chem.* **274,** 33557–33564
33. Ma, H. T., Patterson, R. L., van Rossum, D. B., Birnbaumer, L., Mikoshiba, K., and Gill, D. L. (2000) *Science* **287,** 1647–1651
34. Holda, J. R., and Blatter, L. A. (1997) *FEBS Lett.* **403,** 191–196
35. Pedrosa Ribeiro, C. M., Reece, J., and Putney, J. W., Jr. (1997) *J. Biol. Chem.* **272,** 26555–26561
36. Paradiso, A. M., Mason, S. J., Lazarowski, E. R., and Boucher, R. C. (1995) *Nature* **377,** 643–646
37. Kasai, H., and Petersen, O. H. (1994) *Trends Neurosci.* **17,** 95–101
38. Wakui, M., Potter, B. V., and Petersen, O. H. (1989) *Nature* **339,** 317–320
39. Terasaki, M., Chen, L. B., and Fujiwara, K. (1986) *J. Cell Biol.* **103,** 1557–1568
40. Lee, C., Ferguson, M., and Chen, L. B. (1989) *J. Cell Biol.* **109,** 2045–2055
41. Waterman-Storer, C. M., and Salmon, E. D. (1998) *Curr. Biol.* **8,** 798–806
42. Lane, J. D., and Allan, V. J. (1999) *Mol. Biol. Cell* **10,** 1909–1022
43. Klopfenstein, D. R., Kappeler, F., and Hauri, H. P. (1998) *EMBO J.* **17,** 6168–6177
44. Saraste, J., and Svensson, K. (1991) *J. Cell Sci.* **100,** 415–430
45. Cole, N. B., Sciaky, N., Marotta, A., Song, J., and Lippincott-Schwartz, J. (1996) *Mol. Biol. Cell* **7,** 631–650
46. Duesbery, N. S., and Masui, Y. (1996) *Zygote* **4,** 21–30
47. Tasaka, K., Mio, M., and Izushi, K. (1991) *Skin Pharmacol.* **4,** Suppl. 1, 43–55
48. da Costa, S. R., Yarber, F. A., Zhang, L., Sonee, M., and Hamm-Alvarez, S. F. (1998) *J. Cell Sci.* **111,** 1267–1276
49. Schäfer, C., Ross, S. E., Bragado, M. J., Groblewski, G. E., Ernst, S. A., and Williams, J. A. (1998) *J. Biol. Chem.* **273,** 24173–24180
50. O'Brien, E. T., Salmon, E. D., and Erickson, H. P. (1997) *Cell Motil. Cytoskel.* **36,** 125–135
51. Keith, C., DiPaola, M., Maxfield, F. R., and Shelanski, M. L. (1983) *J. Cell Biol.* **97,** 1918–1924
52. Lee, Y. C., and Wolff, J. (1982) *J. Biol. Chem.* **257,** 6306–6310
53. Craske, M., Takeo, T., Gerasimenko, O., Vaillant, C., Török, K., Petersen, O. H., and Tepikin, A. V. (1999) *Proc. Natl. Acad. Sci. U. S. A.* **96,** 4426–4431

Microtubules Regulate Local Ca^{2+} Spiking in Secretory Epithelial Cells

Kevin E. Fogarty, Jackie F. Kidd, Angelina Turner, Jeremy N. Skepper, Jeff Carmichael and Peter Thorn

J. Biol. Chem. 2000, 275:22487-22494.
doi: 10.1074/jbc.M909402199 originally published online May 8, 2000
